WDS'13 Proceedings of Contributed Papers, Part II, 73–79, 2013. ISBN 978-80-7378-251-1 © MATFYZPRESS

Dust Observation in the COMPASS Tokamak Using Fast Camera

M. Odstrčil,[1,2] J. Mlynář,[3] V. Weinzettl,[3] P. Háček,[3] M. Berta,[4]
T. Szabolics,[5] A. Bencze[5]

[1] Charles University in Prague, Faculty of Mathematics and Physics,
Prague, Czech Republic.
[2] Czech Technical University, Faculty of Nuclear Science and Physical Engineering,
Prague, Czech Republic.
[3] Institute of Plasma Physics, ASCR, Prague, Czech Republic.
[4] Szechenyi Istvan University, Gyor, Hungary.
[5] Institute for Particle and Nuclear Physics, Wigner Research Centre for Physics,
Hungarian Academy of Sciences, Hungary.

Abstract. The dust grains were observed over a thousand discharges in the tokamak COMPASS. A novel method for semi-automatic extraction and tracking of dust grains using a relatively low frame-rate camera (370 fps) was proposed. Radiation lifetime, time evolution and the acceleration of the dust grains were studied. The measured dust velocities roughly correspond to a simple model. However, slow dust particles are significantly affected by local plasma properties and initial release conditions that cannot be determined in our experiment.

Introduction

Dust inside the tokamak vessel can be a serious issue in the future fusion devices such as tokamak ITER [Winter, 1999]. However, even in the present tokamaks, dust can deteriorate plasma parameters. In order to predict dust accumulation, it is necessary to study and model dust production and behavior. Several models were developed for the dust dynamics study in tokamak plasma: the Dust in tokamaks (DTOKS) code [Martin et al., 2008] and DUST Transport (DUSTT) [Pigarov et al., 2005; Smirnov et al., 2011]. Generally, the dust dynamics depends predominantly on the dust–plasma interaction (friction force) in the toroidal direction and on electric force in the radial direction. The dust lifetime is determined by dust grain size, composition and plasma temperature and density [Krasheninnikov et al., 2011]. The dust production is dominated by flaking, brittle destruction of graphite and arcing [Winter, 1999] of the redeposited layers in the case of carbon-based plasma facing components (PFCs).

This work is mainly focused on experimental observation of dust particles in the tokamak COMPASS. Since high speed cameras can provide hundreds of MB data per a shot, it is necessary to develop automatic procedures to extract the dust position. These methods must be (i) fast because the amount of processed data is huge and (ii) robust because number of false event detection needs to be sufficiently low. Our method was focused on data extraction from a relatively slow camera (370 fps) with the read-out time 1.7 ms when the signal is not measured.

In the recent years, many studies focused on dust creating and behavior in tokamaks were published. The concentration, size and composition of the dust particles can be evaluated using *post-mortem* analysis when the dust particles are collected during the chamber vent events. This methods is very important for statistical evaluation over large periods however, it cannot determine the dust dynamics. Another option is to use a fast camera to observe movements of the dust grains [Yu et al., 2009; Rudakov et al., 2009; Hong et al., 2010] inside the vessel. This method allows to estimate dust dynamics but it cannot give information about mass or size of the particles. Finally, many *in-situ* methods were developed such as electrostatic dust detectors, aerogels, laser scattering. These methods can provide valuable information about dust grains hitting the surface of the tokamak vessel.

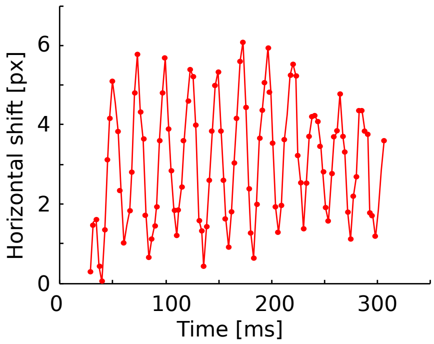

Figure 1. An example of the camera vibrations in the horizontal direction for the shot #3850 caused by mutual motion of the toroidal field coils and the tokamak construction.

Dust Tracking in the Tokamak COMPASS

Our database is based on measurements from the tokamak COMPASS (ASCR, Prague). The major and minor radii of the COMPASS tokamak are 0.56 m and 0.23–0.38 m, respectively, the plasma current is 200–400 kA and the plasma temperature up to 1 keV and the typical discharge length is between 150–300 ms.

The observed plasma was either in the limiter or divertor configuration. Discharges with additional power and torque input from neutral beam injections (NBIs) were not available in our dataset. Therefore, all discharges were in clear L-mode with the ohmic heating.

The dust database was based on a dataset obtained from discharges 2700–3900 corresponding to years 2011–2012. Measurements were performed by the camera EDICAM [Szappanos et al., 2010] that is installed above the mid-plane of the tokamak. The frame resolution was cropped to 902×992 and the frame-rate was estimated to 370 frames per second (fps) with exposure time 1.0 ms and readout time 1.7 ms. The sampled dynamic range is 12 bit, however due to strong readout noise, the effective dynamic range is less than 10 bit.

Data Extraction

Firstly, an image stabilization was performed because vibrations would cause blurring of our background model (next Section). We used an edge enhancement algorithm based on the Sobel operator in combination with normalized cross-correlation

$$\frac{1}{n}\sum_{x,y}\frac{(f(x,y)-\overline{f})(t(x,y)-\overline{t})}{\sigma_f\sigma_t} \quad , \tag{1}$$

where $f(x,y)$ and $t(x,y)$ are edge enhanced original and reference images. The resulting shift for horizontal direction is shown in Fig. 1. The nearest-neighbor interpolation was used for subsequent correction to avoid blurring of the image and changing statistical properties i.e. spreading the X-ray damaged pixels. Fig. 2 shows region used for the cross-correlation with the used mask.

Background Subtraction

The crucial step in the dust particles detection process is a proper background subtraction. The dust radiation can be very weak compared to the background radiation ie. plasma emissivity and the subsequent reflections from the tokamak vessel. Furthermore, long exposure time of the camera along with finite aperture cause blurring of the dust and hence decreasing contrast.

The developed background subtraction method is based on the Randomized Principle Component Analysis (RPCA) [Halko et al., 2011]. The main aim of the method was to use all possible a-priori knowledge about the plasma position and chamber pattern in order to maximize the number of the recognized dust particles. Only “interesting frames,” e. g., frames with

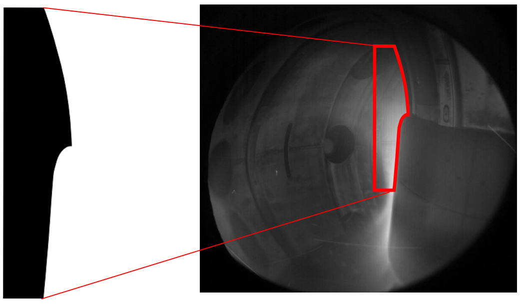

Figure 2. The artificial correlation mask that was used for the image registration (left) and an example of one image frame from the camera (right). The mask corresponds to the center region of the image frame.

non-stationary plasma shape were selected for the final decomposition because the size of the full dataset was 150 GB. The "interesting frames" were detected as frames that were not well described by a first estimation of the RPCA model.

The data matrix I of size $n \times m$ contains the selected set of m images with the resolution n pixels reshaped to columns. I is decomposed using the RPCA

$$I = U\Sigma V^* \quad , \tag{2}$$

where the matrix U is an unitary matrix $m \times k$ (see Fig. 4), Σ is a diagonal matrix $k \times k$ with so called singular values on the diagonal and V is a $n \times k$ unitary matrix. Only the first k singular vectors were computed. The k was estimated from the power spectrum of the matrix Σ. The projection of the original image I to the orthogonal singular vector matrix U was subtracted. Therefore, the background subtracted image I_{sub} is a complement to the low-rank space of the singular vectors

$$I_{\mathrm{sub}} = \left(\mathbb{1} - U^T U\right) I_i \quad , \tag{3}$$

where I_i is the vectorized i-th frame.

Foreground Detection

Candidates for the dust tracks were recognized as blobs exceeding a certain threshold. The image intensity was normalized by local standard deviation σ (in time and space) and by edge enhanced model σ_{edge} (Fig. 3)

$$\frac{I_{\mathrm{sub}}}{\sqrt{\sigma^2 + \sigma^2_{\mathrm{edge}}}} > T_{loc} \quad , \tag{4}$$

where I_{sub} is the background subtracted image. The optimal threshold was estimated by an improved Otsu [1975] method. The edge model (Fig. 3) was determined by an application of an edge enhancement method on the low-rank projection of each frame I_i

$$\sigma_{\mathrm{edge}} = \left(U(UI_i)^T\right) * k \quad , \tag{5}$$

where $*$ denotes convolution and k is the Sobel kernel. The detected objects were further filtered using clustering algorithms in order to separate hotpots and plasma fluctuations. False objects were detected by shape and position similarities compared to the other objects in the database.

The final database contains 11000 dust tracks and 13500 non-dust objects. Reliability of the dust database was estimated by a random selection and manual object checking to be more than 95 %.

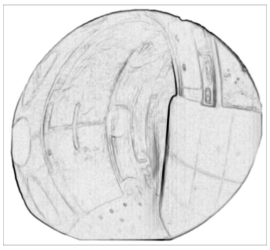

Figure 3. Edge enhanced low-rank projection of one frame with plasma.

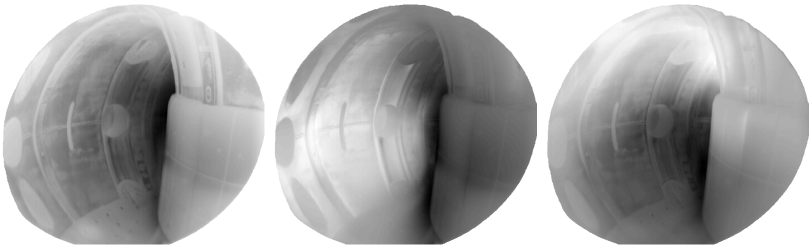

Figure 4. Examples of three main singular vectors ie. the first columns of the matrix U (Eq. 2).

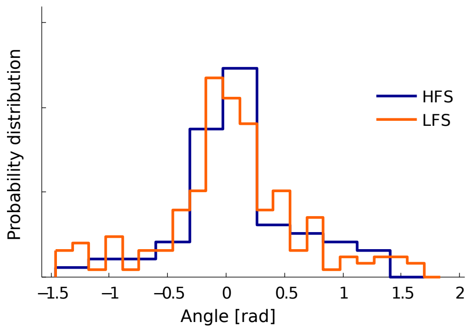

Figure 5. Histogram of dust tracks angle relatively to the toroidal direction of the tokamak.

Results

Two methods were used in order to measure the dust dynamics. The first method obtained the particle velocity and position directly from the dust track shape ie. length L and width W. Each object was fitted with a regularized second order polynomial and width of object W was estimated from the residuum as $2 \cdot 1.48 \cdot MAD$ where MAD is median absolute deviation. The length L_{obj} was estimated as $L_{\mathrm{fit}} - 2W$ in order to remove blurring effects. The length L is directly proportional to 2D projection of 3D velocity while the width W roughly corresponds to the distance from camera due to the finite camera aperture. The dust velocity is equal to

$$v = f\,(L/\tau, x, y) \tag{6}$$

where f is a non-linear geometry transformation correcting the measured 2D projection of the velocity to 3D space. The correction f was calculated numerically for each pixel using a simplifying assumption that radiating dust is observed in a thin shell near to the scrape-of-layer and $\tau = 1.0\,\mathrm{ms}$ is exposure time of our camera.

The resulting velocities are shown in Fig. 6. This direct method is the only way how to estimate velocities of very fast dust particles that are not observable in the subsequent frames. Further, the relative angles of dust tracks compared to the mid-plane (Fig. 5) follows approximately magnetic field although fast particles moving in the perpendicular direction were also observed.

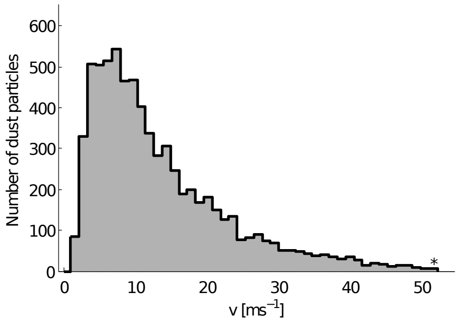

Figure 6. Magnitude of velocity of dust particles on the high field side of the tokamak vessel.

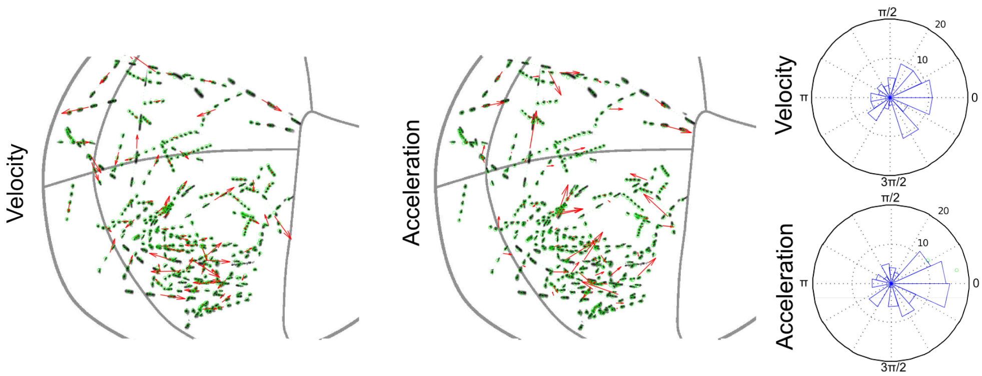

Figure 7. Velocity and acceleration of particles reliably tracked over more than 5 frames at low-field side of the tokamak vessel. Angular distribution shows that particles are preferably moving and accelerating in the toroidal direction.

Slow particles with long survival time were tracked and assigned using a heuristic algorithm. The information about shape, luminosity and velocity of the dust track was used to estimate future position and particle in the following frame that exceeding certain level of similarity was assigned. The optimal combination was searched for a higher number of the candidates. This particles were tracked up to 30 ms. However, the total number of the tracked particles over more than two frame was only 297. Velocity and acceleration were estimated for the most reliable dust tracks and they are shown in Fig. 7. Finally, the number of the dust particles observed per one discharge variated from 5 to 500 with no clear dependence on the plasma shape or tokamak vent events and disruptions.

Discussion

The original 2D projection of the dust tracks were recalculated to a 3D shape using the a-priory knowledge that dust can be observed only in a thin shell near to tokamak wall. The velocity (Fig. 6) was estimated only using the dust particles moving along regions of the vessel that are close to perpendicular to the lines of sight of the camera. Therefore the velocity uncertainty was estimated roughly to 10–20 %. On the other hand, if the radiation lifetime was shorter than the camera exposure time, the resulting velocity was underestimated. Further, precision of the minimal measurable velocity by this non-tracking method is limited by the camera point-spread function to $v \gtrsim 5\,\mathrm{ms}^{-1}$ (see Fig. 6) while the maximal velocity is limited by the low signal to noise ratio (SNR) of the fast tracks and the finite field of view. Finally, small or cold grains were not detected because of too low radiation [Smirnov et al., 2009] compared to background light. This could be significantly improved with a higher camera frame-rate or by spectral filters. However, the EDICAM camera is limited by its slow read-out time of the region of interest [Szappanos et al., 2010].

The measured dust velocities 5–50 m/s are smaller than the values measured in large tokamaks (10–100 m/s). This can be explained by weaker plasma fluxes in SOL and slower plasma rotation due to missing torque force from NBI. Another explanation is that the faster particles were lost because of the lower contrast. The SNR $\sim ID/(v\sigma)$ where I is intensity, D is distance of particle from camera, v denotes velocity and σ is average background radiation. The dust size was in a *ex-situ* measurement estimated to roughly 1 μm. The maximal observed dust lifetime < 30 ms is at the bottom edge of the predicted interval 10^{-2} to 1 s for 1 μm carbon dust [Martin et al., 2005] heated to temperature 1000–3000 K [Smirnov et al., 2009] for edge plasma temperatures from 5–50 eV. The reason can be that the intensively radiating dust particles penetrate deeper to the hot plasma where the particles quickly sublimate.

The slow dust particle study (Fig. 7) suggests that dust in the COMPASS is not produced by abrupt events as disruptions because, on contrary to other tokamaks, no radiating dust particles were observed after the plasma disruption events. The main dust source is probably erosion of the carbon plasma facing components that produce cold dust (invisible for our camera). The dust can be observed after penetration to the SOL where the particles are heated and start to radiate. Average acceleration was estimated only for the well tracked particles during the plasma flat-top phase. The measured acceleration almost constant over the particles tracked time, however the direction of the acceleration was significantly different for each slow particle. Generally, the particles were preferably accelerated in the toroidal direction (Fig. 7). The fast particles are clearly accelerated in the direction of the plasma rotation (see Fig. 5). The SOL plasma velocity is not routinely measured in the COMPASS tokamak and the initial measurements only suggests that the poloidal boundary plasma velocity is below 2 km/s.

Conclusion

The observed dust velocity in the tokamak COMPASS was between 5–50 m/s with lifetime of the radiating stage less than 30 ms. No clear sources of dust were observed so the dust is expected to be created by PFC erosion during regular tokamak operation. The slow dust particles dynamics was inconclusive. In future, it is necessary to measure more dust particles with a higher time resolution and determine the boundary plasma properties in order to apply models for dust behavior.

Acknowledgments. This work was supported by MSMT Project #LM2011021 and carried out within the framework of the European Fusion Development Agreement. The views and opinions expressed herein do not necessarily reflect those of the European Commission.

References

Halko, N., Martinsson, P.-G., Shkolnisky, Y., and Tygert, M., An Algorithm for the Principal Component Analysis of Large Data Sets., *SIAM Journal on Scientific Computing*, 2011.

Hong, S.-H., Grisolia, C., Rohde, V., Monier-Garbet, P., Team, T., and Team, A., Temporal evolution and spatial distribution of dust creation events in Tore Supra and in ASDEX Upgrade studied by CCD image analysis, *Nuclear Fusion*, 2010.

Krasheninnikov, S., Smirnov, R., and Rudakov, D., Dust in magnetic fusion devices, *Plasma Physics and Controlled Fusion*, 2011.

Martin, J., Coppins, M., and Counsell, G., Motion and lifetime of dust grains in a tokamak plasma, *Journal of nuclear materials*, 2005.

Martin, J., Bacharis, M., Coppins, M., Counsell, G., and Allen, J., Modelling dust transport in tokamaks, *Europhysics Letters*, 2008.

Otsu, N., A threshold selection method from gray-level histograms, *Automatica*, 1975.

Pigarov, A. Y., Krasheninnikov, S., Soboleva, T., and Rognlien, T., Dust-particle transport in tokamak edge plasmas, *Physics of plasmas*, 2005.

Rudakov, D., Litnovsky, A., West, W., Yu, J., Boedo, J., Bray, B., Brezinsek, S., Brooks, N., Fenstermacher, M., Groth, M., et al., Dust studies in DIII-D and TEXTOR, *Nuclear Fusion*, 2009.

Smirnov, R., Krasheninnikov, S., Yu, J., Pigarov, A. Y., Rosenberg, M., and Terry, J., On visibility of carbon dust particles in fusion plasmas with fast framing cameras, *Plasma Physics and Controlled Fusion*, 2009.

Smirnov, R., Krasheninnikov, S., Pigarov, A. Y., Roquemore, A., Mansfield, D., and Nichols, J., Modeling of dust impact on tokamak edge plasmas, *Journal of Nuclear Materials*, 2011.

Szappanos, A., Berta, M., Hron, M., Pánek, R., Stöckel, J., Tulipán, S., Veres, G., Weinzettl, V., and Zoletnik, S., EDICAM fast video diagnostic installation on the COMPASS tokamak, 2010.

Winter, J., Dust in fusion devices-experimental evidence, possible sources and consequences, *Plasma physics and controlled fusion*, 1999.

Yu, J., Rudakov, D., Pigarov, A. Y., Smirnov, R., Brooks, N., Muller, S., and West, W., Fast camera imaging of dust in the DIII-D tokamak, *Journal of Nuclear Materials*, 2009.